



| | |
|------------------------|---|
| Title | Two types of quasi-liquid layers on ice crystals are formed kinetically |
| Author(s) | Asakawa, Harutoshi; Sazaki, Gen; Nagashima, Ken; Nakatsubo, Shunichi; Furukawa, Yoshinori |
| Citation | Proceedings of the National Academy of Sciences of the United States of America, 113(7), 1749-1753 https://doi.org/10.1073/pnas.1521607113 |
| Issue Date | 2016-02-16 |
| Doc URL | http://hdl.handle.net/2115/62688 |
| Type | article (author version) |
| Additional Information | There are other files related to this item in HUSCAP. Check the above URL. |
| File Information | Manuscript-Sazaki-R1.pdf |



[Instructions for use](#)

Classification: Physical Sciences (Physics)

Two types of quasi-liquid layers on ice crystals are formed kinetically

Harutoshi Asakawa[†], Gen Sazaki^{*}, Ken Nagashima,, Shunichi Nakatsubo, Yoshinori Furukawa

Institute of Low Temperature Science, Hokkaido University, N19-W8, Kita-ku, Sapporo 060-0819, Japan

Author contributions: H.A., G.S. and Y.F. designed the research; H.A., G.S. and K.N. performed research; S.N. produced the experimental system; H.A. and G.S. wrote the paper.

The authors declare no conflict of interest.

[†] Present address: Department of Creative Technology Engineering, National Institute of Technology, Anan College, 265 Aoki Minobayashi, Anan, Tokushima 774-0017, Japan

^{*} To whom correspondence should be addressed. E-mail: sazaki@lowtem.hokudai.ac.jp

Key words: molecular-level observation, advanced optical microscopy, metastable phase

Abstract

Surfaces of ice are covered with thin liquid water layers, called quasi-liquid layers (QLLs), even below their melting point ($0\text{ }^{\circ}\text{C}$), which govern a wide variety of phenomena in nature. We recently found that two types of QLL phases appear that exhibit different morphologies (droplets and thin layers) (Sazaki G. *et al.* (2012) Quasi-liquid layers on ice crystal surfaces are made up of two different phases. *Proc. Natl. Acad. Sci. USA* 109: 1052–1055). However, revealing the thermodynamic stabilities of QLLs remains a longstanding elusive problem. Here we show that both types of QLLs are metastable phases that appear only if the water vapor pressure is higher than a certain critical supersaturation. We directly visualized the QLLs on ice crystal surfaces by advanced optical microscopy, which can detect 0.37-nm-thick elementary steps on ice crystal surfaces. At a certain fixed temperature, as the water vapor pressure decreased, thin-layer QLLs first disappeared, and then droplet QLLs vanished next, although elementary steps of ice crystals were still growing. These results clearly demonstrate that both types of QLLs are kinetically formed, not by the melting of ice surfaces, but by the deposition of supersaturated water vapor on ice surfaces. This appears to be the first experimental evidence that supersaturation of water vapor plays a crucially important role in the formation of QLLs.

Significance statement

Thin liquid water layers, so-called "quasi-liquid layers" (QLLs), exist on ice surfaces just below the melting point (0°C). The formation of QLLs governs various important phenomena on the earth, such as weather- and environment-related issues, winter sports, etc. Hence, QLLs have attracted considerable attention in the fields of ice physics, meteorology, crystal growth and surface science. Our molecular-level observation of QLLs by advanced optical microscopy revealed that QLLs are formed kinetically as metastable phases only in supersaturated water vapor. This finding opens new horizons of understanding QLLs, which have been so far discussed thermodynamically only at an equilibrium condition.

/body

Introduction

Ice is one of the most abundant materials on the Earth, and its surfaces are covered with thin liquid water layers even below their melting point (0 °C) (1-4). Such thin liquid water layers are called “quasi-liquid layers” (QLLs). Since QLLs govern the surface properties of ice just below the melting point, it is well acknowledged that surface melting of ice governs a wide variety of phenomena, such as electrification of thunderclouds (4, 5), regelation (4, 6), frost heave (4, 7), conservation of foods, ice-skating (1, 8), preparation of a snow man (1), and growth of ice crystals (2, 4). Therefore, it is essential to understand the surface melting of ice crystals at the molecular level.

After Michael Faraday proposed the existence of QLLs in 1842 (1), many studies experimentally confirmed the formation of QLLs by various methods (See table S1). All of such studies revealed that the thickness of QLLs significantly increases with increasing temperature. However, such the studies utilized spectroscopy and scattering methods, which can obtain only temporally- and spatially-averaged information, or optical microscopy, which does not have sufficient spatial resolution. Hence, the nature of surface melting has not been fully unlocked. To further understand the dynamic behavior of QLLs, we need to perform real-time and real-space observations of ice crystal surfaces at the molecular level.

Recently, we and Olympus Engineering Co., Ltd. have developed one such technique - namely, laser confocal microscopy combined with differential interference contrast microscopy (LCM-DIM) (9), which can directly visualize the 0.37-nm-thick elementary steps on ice crystal surfaces (10, 11). We found that two types of QLL phases with different morphologies appear (12-14): round liquid-like drops (α -QLLs) and thin liquid-like layers (β -QLLs) emerge, irrespective of the face indices of the ice surfaces. Until our recent studies were reported, it had been believed for many years that only one QLL phase appears in the conventional picture of surface melting (2-4). Hence, our results demonstrate that the conventional picture needs important re-examination.

However, it is still unclear how we can explain the generation of the two types of QLL phases. To approach this issue, we first focused our attention on the thermodynamic stabilities of the two types of QLLs. In this study, we examined a water vapor pressure range in which the two types of QLL phases appeared on ice basal faces by LCM-DIM. As a result, we found that the two types of QLL phases are metastable phases that appear only when the water vapor pressure is higher than a certain critical supersaturation.

Results and Discussion

We prepared an observation chamber (Fig. S1) in which the temperature of sample ice crystals T_{sample} and the partial pressure of water vapor $P_{\text{H}_2\text{O}}$ can be separately controlled. We kept the total pressure in the chamber at atmospheric pressure using nitrogen gas, and changed the degree of supersaturation of water vapor $\sigma=(P_{\text{H}_2\text{O}} - P_e)/P_e$ by changing $P_{\text{H}_2\text{O}}$ (here P_e is the solid–vapor equilibrium pressure). We grew Ih ice single crystals on a cleaved AgI crystal (Fig. S1) at $T_{\text{sample}}=-15.0$ °C and $P_{\text{H}_2\text{O}}=585$ Pa ($\sigma=13$ %) in a nitrogen environment. After the preparation of ice single crystals, we increased T_{sample} to a given temperature. All through this process, we kept the sample ice crystals growing, by carefully changing $P_{\text{H}_2\text{O}}$ and confirming the growth by LCM-DIM observations. Then, we observed the behavior of QLLs on basal faces of sample ice crystals under various $P_{\text{H}_2\text{O}}$ (σ) conditions. LCM-DIM images were processed according to the recipe explained in Fig. S2. Details of the control of T_{sample} and $P_{\text{H}_2\text{O}}$ were explained in our previous publication (15).

To reveal the thermodynamic stabilities of the two types of QLL phases, we investigated the water vapor pressure range in which the two types of QLLs could exist on ice basal faces. After we changed T_{sample} and $P_{\text{H}_2\text{O}}$ from -2.4 °C and 585 Pa ($\sigma=13$ %) into -2.0 °C and 585 Pa ($\sigma=13$ %), both α - and β -QLL phases appeared on a bare ice basal face. Fig. 1 and Video S1 show the ice basal face after the change. In Fig. 1, white and half-black/white arrowheads represent α - and β -QLLs, respectively. The black arrowhead (Fig. 1A) depicts an elementary step (0.37 nm in height) growing laterally in the direction of the black arrow (10, 11, 15). In this study, the differential interference contrast was adjusted as if the ice crystal surface were illuminated by a light beam slanted from the upper left to the lower-right direction (Fig. S3). Hence, the upper left sides and the lower right sides of convex objects showed brighter and darker contrast compared to a flat crystal surface, respectively. As marked by white arrowheads in Figs. 1B and C, α -QLLs newly appeared on a β -QLL phase. In addition, adjacent β -QLLs coalesced with each other (half-black/white arrowheads in Figs. 1B and C), and then β -QLLs grew in the lateral direction.

Next, we reduced $P_{\text{H}_2\text{O}}$ to 568 Pa (to $\sigma=10$ %) while keeping T_{sample} constant at -2.0 °C, and observed how the two types of QLLs behaved by LCM-DIM (Fig. 2 and Video S2). The arrowheads and arrows have the same meaning as those in Fig. 1. Elementary steps (black arrowheads) grew laterally in the direction of the black arrow. However, under this condition, the β -QLL (half-black/white arrowheads) receded gradually. Finally the β -QLL disappeared completely (Figs. 2C and D), although α -QLLs (white arrowheads)

remained stable.

Then, we further reduced $P_{\text{H}_2\text{O}}$ to 532 Pa (to $\sigma=3\%$), keeping T_{sample} constant at $-2.0\text{ }^\circ\text{C}$, and observed the behavior on the ice basal face. Fig. 3 and Video S3 show the result. The elementary step marked by the black arrowhead in Fig. 3E grew laterally in the black arrow direction, and then reached the position marked by the black arrowhead in Fig. 3F. Hence, we could confirm that $P_{\text{H}_2\text{O}}$ was definitely in a supersaturated condition ($\sigma>0$). However, the α -QLL in Fig. 3 (white arrowheads) became gradually smaller as time elapsed. Then 2 hours after Fig. 3A was taken, the α -QLL disappeared completely.

In Figs. 1-3, we examined the critical $P_{\text{H}_2\text{O}}$ above which α - and β -QLLs could appear, keeping T_{sample} constant at $-2.0\text{ }^\circ\text{C}$. We performed similar observations at various T_{sample} to determine the pressure-temperature range in which two types of QLLs could grow. We summarize the results in Fig. 4. Blue filled circles and red open rhombuses show the minimum $P_{\text{H}_2\text{O}}$ at which α - and β -QLLs could appear, respectively (blue and red solid lines are guides for eyes). In other words, α - and β -QLLs could exist only under $P_{\text{H}_2\text{O}}$ conditions higher than these respective plots. Black open squares present the solid-vapor equilibrium $P_{\text{H}_2\text{O}}$ that we determined experimentally from the LCM-DIM observations of the growth and recession of elementary steps and crystal edges (15). Solid and dashed black curves in Fig. 4 show the solid-vapor equilibrium $P_{\text{H}_2\text{O}}$ and the liquid-vapor equilibrium $P_{\text{H}_2\text{O}}$, respectively, obtained in previous studies (16, 17). The dash-dotted black line also represents the solid-liquid equilibrium $P_{\text{H}_2\text{O}}$ obtained from a calculation using the molar volumes of water and ice, the melting point, and the heat of fusion of ice crystals (18). Fig. 4 clearly demonstrates that even just below the melting point, α - and β -QLLs appeared only when $P_{\text{H}_2\text{O}}$ was supersaturated for both ice crystals and liquid water. From this result, we proved, for the first time, that α - and β -QLLs are thermodynamically metastable phases. We also found that β -QLLs could appear only in a higher $P_{\text{H}_2\text{O}}$ range than α -QLLs: β -QLLs are less stable than α -QLLs.

Many researchers so far experimentally examined the formation of QLLs under various conditions using different techniques (for detail see Table S1). Some reported that QLLs were formed with $P_{\text{H}_2\text{O}}$ corresponding to an undersaturated condition, and some others reported the formation of QLLs under an equilibrium or supersaturated condition. Hence, until we performed the present experiments, there was not a unified view about the role of supersaturation. Moreover, as we reported previously (Fig. S3 of reference (15)), it is not easy to accurately evaluate the supersaturation of $P_{\text{H}_2\text{O}}$ in the vicinity of a growing or sublimating ice crystal. In our new work, we evaluated the supersaturation of $P_{\text{H}_2\text{O}}$ by directly observing the growth and recession of elementary steps. Hence, we believe that we have evaluated the degree of supersaturation more accurately than the

other experiments performed so far, and that the results shown in Fig. 4 are substantive. In the conventional picture of surface melting, it had been thought that only one QLL phase fully covers an ice surface at the solid-vapor equilibrium $P_{\text{H}_2\text{O}}$ (2-4). Lacmann and Stranski first gave a thermodynamic explanation for the wetting of ice crystal surfaces with QLLs (19). Then Kuroda and Lacmann developed this issue into the explanation of morphologies of snowflakes (2). Their theoretical model is based on the competition between the stabilities of a bulk (unstable) and interfaces (stable) of QLLs at the equilibrium $P_{\text{H}_2\text{O}}$ (for details see Fig. S4) (2). Kuroda and Lacmann evaluated the wettability of a QLL on ice crystal surfaces utilizing values of interfacial free energies determined previously (2, 18, 20), which lead them to expect that an ice crystal surface is fully wetted with a QLL (2). Taking into account the contributions of a bulk (unstable) and interfaces (stable) of a QLL, Kuroda and Lacmann assumed that a QLL and an ice can be in equilibrium at the solid-vapor equilibrium $P_{\text{H}_2\text{O}}$, as schematically shown in Fig. 5A. In addition, taking into account the effects of kinetics, they also presumed that a QLL can exist under both undersaturated and supersaturated $P_{\text{H}_2\text{O}}$ conditions (Fig. 5A).

In Fig. 5B, we also summarized the supersaturation range in which the two types of QLLs appeared in our experiments. In contrast to the conventional picture (Fig. 5A), at equilibrium $P_{\text{H}_2\text{O}}$, we found that no QLL phase appeared on ice crystal surfaces. This discrepancy was mainly due to the misestimation of free energy of an ice-vapor interface by Kuroda and Lacmann, who estimated the ice-vapor interfacial free energy from the density of dangling bonds on ice crystal surfaces. However, at ultra-high temperatures (just below the melting point), the effects of entropy significantly decrease the interfacial free energy. Hence, they overestimated the ice-vapor interfacial free energy, leading to the complete wetting of ice crystal surfaces with QLLs (Fig. 5A). Since we can directly observe two-dimensional (2D) nucleation on an ice crystal surface by LCM-DIM (10, 11), we plan to accurately evaluate the ice-vapor interfacial free energy from the measurement of 2D nucleation rates in the future.

In addition to the situation for equilibrium $P_{\text{H}_2\text{O}}$, we found that no QLL phase appeared on ice crystal surfaces under both undersaturated and low supersaturated $P_{\text{H}_2\text{O}}$ conditions (Fig. 5B). QLLs appeared only for $P_{\text{H}_2\text{O}}$ higher than a certain critical supersaturation. This result clearly demonstrates that QLL phases are less stable than ice in any $P_{\text{H}_2\text{O}}$ range. In other words, two types of QLLs are formed kinetically, not by the melting of ice surfaces, but by the deposition of supersaturated water vapor on ice surfaces. To our knowledge, this study shows the first experimental evidence that supersaturation of water vapor plays a crucially important role in the formation of

QLLs.

In addition, the two types of QLLs exhibited different stabilities. As demonstrated in this study, β -QLLs appear at a $P_{\text{H}_2\text{O}}$ significantly higher than α -QLLs: the stability of β -QLLs is notably lower than that of α -QLLs. Nevertheless, β -QLLs show a much flatter shape than α -QLLs, implying that β -QLLs have more favorable interaction (*i.e.* better wettability) with ice surfaces than α -QLLs. To solve this contradiction, we need to obtain more information about the structures of α - and β -QLLs. Hence, we are developing a Raman spectrometer combined with LCM-DIM.

The kinetics of the growth and reduction of α - and β -QLLs is very important. However, to obtain meaningful kinetic data, we need to measure separately the mass transfer processes of water molecules (1) between water vapor and QLLs, (2) between QLLs and ice surfaces (effects of QLLs on the growth of ice crystals) and (3) between α - and β -QLLs. At present, we have no practical idea how to measure the processes (1)-(3). Hence, the elucidation of these processes is a major challenge for the future.

In this study, we performed in-situ LCM-DIM observations on ice basal faces to examine the range of $P_{\text{H}_2\text{O}}$ in which α - and β -QLLs emerged. As a result, we found that α - and β -QLLs are metastable phases that can appear only if $P_{\text{H}_2\text{O}}$ is higher than a critical supersaturation. This result indicates that the two types of QLLs are kinetically formed, not by the melting of ice surfaces, but by the deposition of supersaturated water vapor on ice surfaces. Our findings will provide a key to unlocking the secrets of the various phenomena related with surface melting, from the electrification of thunderclouds to the growth of ice crystals (4).

Material and method

A confocal system (FV300, Olympus Optical Co. Ltd.) was attached to an inverted optical microscope (IX70, Olympus Optical Co. Ltd.), as explained in our recent studies (9, 10). A super luminescent diode (Amonics Ltd., model ASLD68-050-B-FA: 680 nm) was used as a light source for the LCM-DIM observations. The LCM-DIM system (Fig. S1) used in this study included a large number of the improvements for the molecular-level observation of ice crystal surfaces under atmospheric pressure (10).

The observation chamber had upper and lower Cu plates, whose temperatures were separately controlled, using Peltier elements (Fig. S1B). At the center of the upper Cu plate, a cleaved AgI crystal (a kind gift from emeritus professor G. Layton of Northern Arizona University), well-known as an ice nucleating agent, was attached using heat grease. On this AgI crystal, the sample ice crystals were grown at -15°C . To supply water vapor to the sample ice crystals, other ice crystals were grown on the lower Cu plate as a source of water vapor. The temperature of the sample ice crystals T_{sample} was determined by controlling the temperature of the upper Cu plate. Since the volume of the source ice crystals on the lower Cu plate was approximately 10^2 times larger than that of the sample ice crystals, the partial pressure of water vapor $P_{\text{H}_2\text{O}}$ inside the observation chamber was dominated by the equilibrium pressure of the source ice crystals. Hence, $P_{\text{H}_2\text{O}}$ was determined by controlling the temperature of the source ice crystals T_{source} (the temperature of the lower Cu plate). Other details, including the calibration of T_{sample} and $P_{\text{H}_2\text{O}}$, were reported in our recent study (15).

Acknowledgements

The authors thank Y. Saito, S. Kobayashi and K. Ishihara (Olympus Engineering Co., Ltd.) for their technical support of LCM-DIM, G. Layton (Northern Arizona University) for the provision of AgI crystals, A.A. Chernov (Lawrence Livermore National Laboratory), H. Nada (AIST), N. Akutsu (Osaka Electro-Communication University) and K. Murata (Hokkaido University) for valuable discussions. G.S. is grateful for the partial support by JSPS KAKENHIs (Grants Nos. 23246001 and 15H02016).

References

1. Faraday M (1850) On certain conditions of freezing water. *Athenaeum* 1181:640-641.
2. Kuroda T & Lacmann R (1982) Growth kinetics of ice from the vapour phase and its growth forms. *J. Cryst. Growth* 56(1):189-205.
3. Chernov AA (1993) Roughening and melting of crystalline surfaces. *Prog. Cryst. Growth Charact.* 26(0):195-218.

4. Dash JG, Rempel AW, & Wettlaufer JS (2006) The physics of premelted ice and its geophysical consequences. *Rev. Mod. Phys.* 78(3):695-741.
5. MacGorman DR & Rust WD (1998) *The electrical nature of storms* (Oxford University Press).
6. Gilpin RR (1980) Wire Regelation at Low-Temperatures. *J. Colloid Interface Sci.* 77(2):435-448.
7. Dash JG (1989) Thermomolecular Pressure in Surface Melting: Motivation for Frost Heave. *Science* 246(4937):1591-1593.
8. Wettlaufer JS & Dash JG (2000) Melting below zero. *Sci. Am.* 282(2):50.
9. Sazaki G, *et al.* (2004) In situ observation of elementary growth steps on the surface of protein crystals by laser confocal microscopy. *J. Cryst. Growth* 262(1-4):536-542.
10. Sazaki G, Zepeda S, Nakatsubo S, Yokoyama E, & Furukawa Y (2010) Elementary steps at the surface of ice crystals visualized by advanced optical microscopy. *Proc. Natl. Acad. Sci. USA* 107(46):19702-19707.
11. Sazaki G, Asakawa H, Nagashima K, Nakatsubo S, & Furukawa Y (2014) Double Spiral Steps on Ih Ice Crystal Surfaces Grown from Water Vapor Just below the Melting Point. *Cryst. Growth Des.* 14(5):2133-2137.
12. Sazaki G, Zepeda S, Nakatsubo S, Yokomine M, & Furukawa Y (2012) Quasi-liquid layers on ice crystal surfaces are made up of two different phases. *Proc. Natl. Acad. Sci. USA* 109(4):1052-1055.
13. Sazaki G, Asakawa H, Nagashima K, Nakatsubo S, & Furukawa Y (2013) How do Quasi-Liquid Layers Emerge from Ice Crystal Surfaces? *Cryst Growth Des.* 13(4):1761-1766.
14. Asakawa H, *et al.* (2015) Prism and Other High-Index Faces of Ice Crystals Exhibit Two Types of Quasi-Liquid Layers. *Cryst Growth Des.* 15(7):3339-3344.
15. Asakawa H, *et al.* (2014) Roles of Surface/Volume Diffusion in the Growth Kinetics of Elementary Spiral Steps on Ice Basal Faces Grown from Water Vapor. *Cryst. Growth Des.* 14(7):3210-3220.
16. Sonntag D (1990) Important new values of the physical constants of 1986, vapour pressure formulations based on the ITS-90, and psychrometer formulae. *Meteorol. Z.* 70(5):340-344.
17. Murphy DK, T. (2005) Review of the vapour pressures of ice and supercooled water for atmospheric applications. *Q. J. Meteorol Soc.* 131(608):1539-1565.
18. Petrenko VF & Whitworth RW (1999) *Physics of ice* (Oxford University Press, Oxford).
19. Lacmann R & Stranski IN (1972) The growth of snow crystals. *J. Cryst. Growth*

- 13:236-240.
20. Hardy S (1977) A grain boundary groove measurement of the surface tension between ice and water. *Phil. Mag.* 35(2):471-484.
 21. Furukawa Y (2015) 25 - Snow and Ice Crystal Growth. *Handbook of Crystal Growth (Second Edition)*, ed Nishinaga T (Elsevier, Boston), pp 1061-1112.
 22. Kino GS & Corle TR (1996) *Confocal scanning optical microscopy and related imaging systems* (Academic Press).
 23. Furukawa Y, Yamamoto M, & Kuroda T (1987) Ellipsometric study of the transition layer on the surface of an ice crystal. *J. Cryst. Growth* 82(4):665-677.
 24. Golecki I & Jaccard C (1977) The surface of ice near 0 C studied by 100 keV proton channeling. *Phys. Lett. A* 63(3):374-376.
 25. Golecki I & Jaccard C (1978) Intrinsic surface disorder in ice near the melting point. *J. Phys. C* 11(20):4229-4237.
 26. Frenken JWM, Marée PMJ, & van der Veen JF (1986) Observation of surface-initiated melting. *Phys. Rev. B* 34(11):7506-7516.
 27. Pluis B, van der Gon AWD, Frenken JWM, & van der Veen JF (1987) Crystal-Face Dependence of Surface Melting. *Phys. Rev. Lett.* 59(23):2678-2681.
 28. Beaglehole D & Nason D (1980) Transition layer on the surface on ice. *Surf. Sci.* 96(1):357.
 29. Kouchi A, Furukawa Y, & Kuroda T (1987) X-ray-diffraction pattern of quasi-liquid layer on ice crystal-surface. *J. Phys. (Paris)* 48:675-677.
 30. Dosch H, Lied A, & Bilgram JH (1995) Glancing-angle X-ray scattering studies of the premelting of ice surfaces. *Surf. Sci.* 327(1-2):145-164.
 31. Dosch H, Lied A, & Bilgram JH (1996) Disruption of the hydrogen-bonding network at the surface of Ih ice near surface premelting. *Surf. Sci.* 366(1):43-50.
 32. Maruyama M, Bienfait M, Dash J, & Coddens G (1992) Interfacial melting of ice in graphite and talc powders. *J. Cryst. Growth* 118(1):33-40.
 33. Nason D & Fletcher N (1975) Photoemission from ice and water surfaces: Quasiliquid layer effect. *J. Chem. Phys.* 62(11):4444-4449.
 34. Bluhm H, Ogletree DF, Fadley CS, Hussain Z, & Salmeron M (2002) The premelting of ice studied with photoelectron spectroscopy. *J. Phys. Condens. Matter* 14(8):L227.
 35. Kvlividze V, Kiselev V, Kurzaev A, & Ushakova L (1974) The mobile water phase on ice surfaces. *Surf. Sci.* 44(1):60-68.
 36. Mizuno Y & Hanafusa N (1987) Studies of surface properties of ice using nuclear magnetic resonance. *J. Phys. (France)* 48(C1):C1-511-C511-517.
 37. Gonda T, Arai T, & Sei T (1999) Experimental study on the melting process of ice

- crystal just below the melting point. *Polar Meteorology and Glaciology* 13:38-42.
38. Elbaum M, Lipson SG, & Dash JG (1993) Optical study of surface melting on ice. *J. Cryst. Growth* 129(3-4):491-505.
 39. Kaverin A, *et al.* (2004) A novel approach for direct measurement of the thickness of the liquid-like layer at the ice/solid interface. *J. Phys. Chem. B* 108(26):8759-8762.
 40. Sadtchenko V & Ewing GE (2003) A new approach to the study of interfacial melting of ice: infrared spectroscopy. *Can. J. Phys.* 81(1-2):333-341.
 41. Wei X, Miranda PB, & Shen YR (2001) Surface Vibrational Spectroscopic Study of Surface Melting of Ice. *Phys. Rev. Lett.* 86(8):1554-1557.
 42. Wei X, Miranda PB, Zhang C, & Shen YR (2002) Sum-frequency spectroscopic studies of ice interfaces. *Phys. Rev. B* 66(8):085401.
 43. Petrenko VF (1997) Study of the Surface of Ice, Ice/Solid and Ice/Liquid Interfaces with Scanning Force Microscopy. *J. Phys. Chem. B* 101(32):6276-6281.
 44. Bluhm H & Salmeron M (1999) Growth of nanometer thin ice films from water vapor studied using scanning polarization force microscopy. *J. Chem. Phys.* 111(15):6947-6954.
 45. Salmeron M & Bluhm H (1999) Structure and properties of ice and water film interfaces in equilibrium with vapor. *Surf. Rev. Lett.* 6(06):1275-1281.
 46. Döppenschmidt A & Butt H-J (2000) Measuring the Thickness of the Liquid-like Layer on Ice Surfaces with Atomic Force Microscopy. *Langmuir* 16(16):6709-6714.

Figures legends

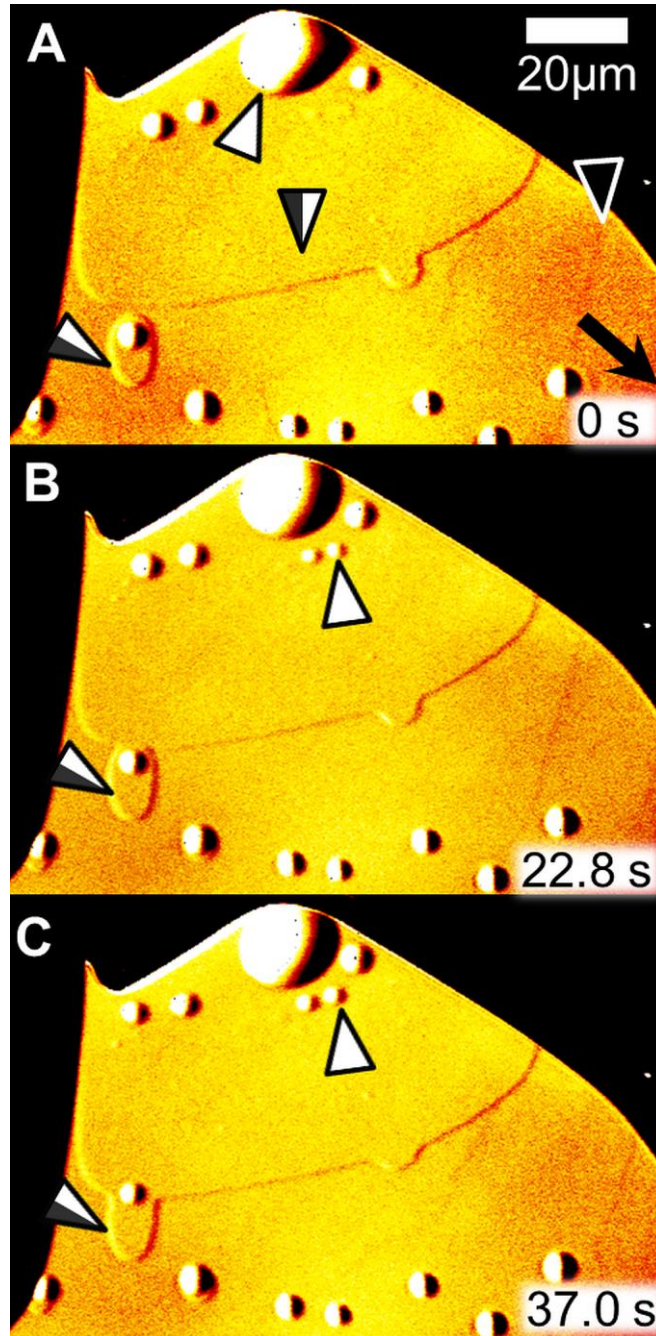


Fig. 1. The appearance of round liquid-like droplets (α -QLLs) and thin liquid-like layers (β -QLLs) on an ice basal face under relatively high supersaturation conditions ($P_{\text{H}_2\text{O}}=585$ Pa, $\sigma=13$ %) at $T_{\text{sample}}=-2.0$ °C. Images B and C were taken 22.8 and 37.0 s after image A, respectively. White and half-black/white arrowheads show α - and β -QLL phases, respectively. A black arrowhead represents an elementary step growing laterally in the black-arrow direction. A movie of the process A-C is available as Video S1.

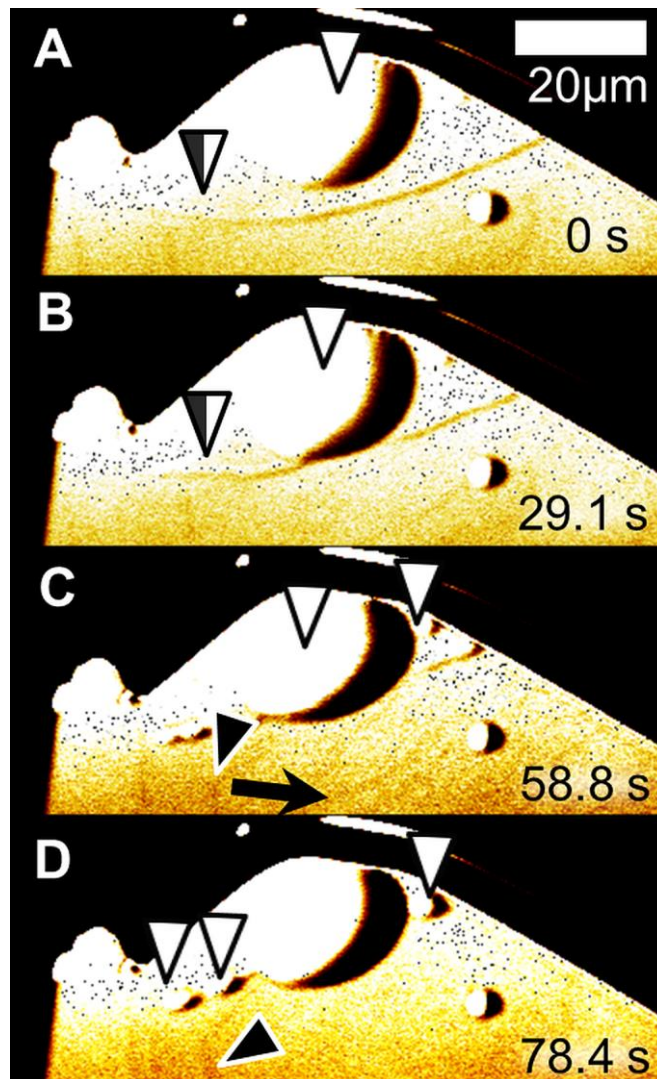


Fig. 2. The disappearance of a thin liquid-like layer (β -QLL) on an ice basal face under relatively medium supersaturation conditions ($P_{\text{H}_2\text{O}}=568$ Pa, $\sigma=10$ %) at $T_{\text{sample}}=-2.0$ °C. After Fig. 1 was taken, $P_{\text{H}_2\text{O}}$ was reduced from 585 to 568 Pa, keeping T_{sample} constant. Images B, C, and D were taken 29.1 s, 58.8 s, and 78.4 s after image A, respectively. White and half-black/white arrowheads show α - and β -QLL phases, respectively. Black arrowheads represent elementary steps growing laterally in the black-arrow direction. A movie of the process A-D is available as Video S2.

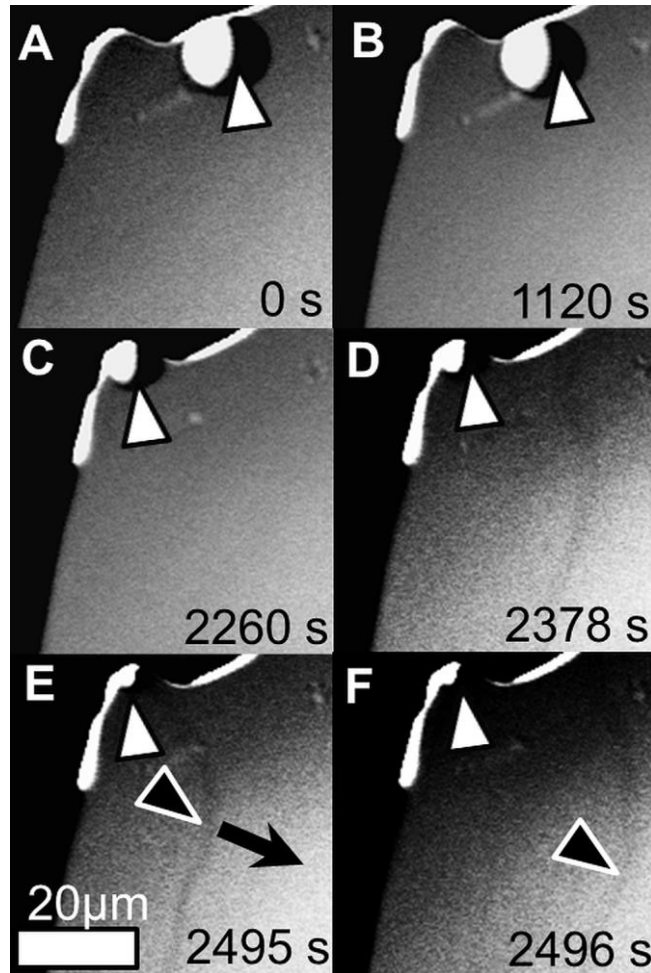


Fig. 3. The disappearance of a round liquid-like droplet (α -QLL) on an ice basal face under relatively low supersaturation conditions ($P_{\text{H}_2\text{O}}=532$ Pa, $\sigma=3$ %) at $T_{\text{sample}}=-2.0$ °C. After Fig. 2 was taken, $P_{\text{H}_2\text{O}}$ was reduced from 568 to 532 Pa, keeping T_{sample} constant. Images B, C, D, E and F were taken 1120 s, 2260 s, 2378 s, 2495 s, and 2496 s after image A, respectively. White arrowheads show α -QLL phases. The elementary step marked by the black arrowhead in E grew laterally in the black arrow direction, and then reached the position marked by the black arrowhead in F. A movie of the process A-F is available as Video S3.

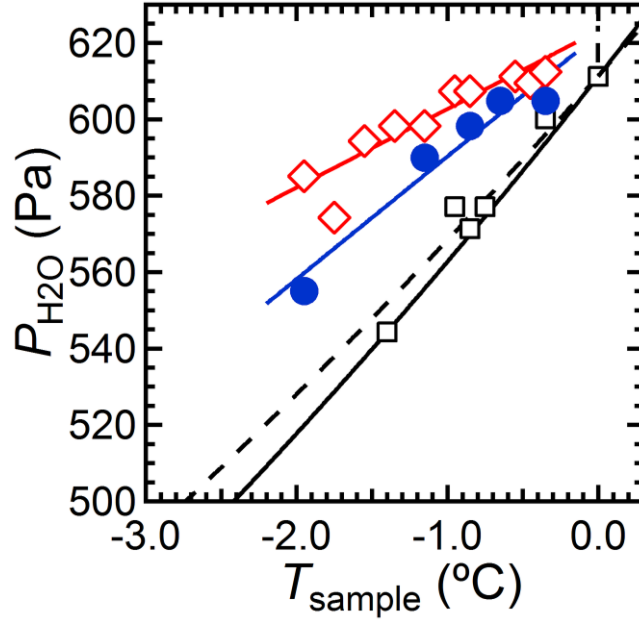


Fig. 4. Pressure-temperature regions in which round liquid-like droplets (α -QLLs) and thin liquid-like layers (β -QLLs) could grow. Blue filled circles and red open rhombuses show the minimum $P_{\text{H}_2\text{O}}$ at which α - and β -QLLs could appear, respectively: α - and β -QLLs could exist only when $P_{\text{H}_2\text{O}}$ is higher than the respective plots. Blue and red solid lines are guides for the eyes. Black open squares presents the solid-vapor equilibrium $P_{\text{H}_2\text{O}}$ that we obtained experimentally from the LCM-DIM observations of the growth and recession of elementary steps and crystal edges (15). Solid and dashed black curves show the solid-vapor equilibrium $P_{\text{H}_2\text{O}}$ and the liquid-vapor equilibrium $P_{\text{H}_2\text{O}}$, respectively, obtained in the previous studies (16, 17). The dash-dotted black line also represents the solid-liquid equilibrium $P_{\text{H}_2\text{O}}$ obtained from the calculation, using the values shown in ref. 18.

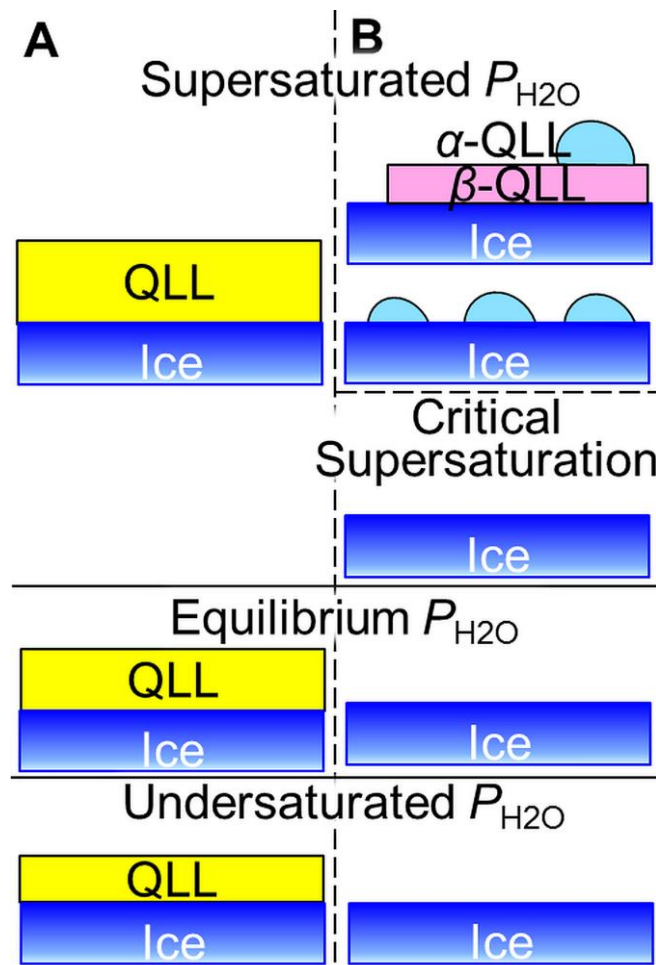


Fig. 5. A comparison between the conventional picture of surface melting (2, 21)(A) and the findings obtained in this study (B). In the conventional picture, one QLL phase appeared irrespective of supersaturation. In contrast, round liquid-like droplets (α -QLLs) and thin liquid-like layers (β -QLLs) appeared only under P_{H_2O} conditions higher than the critical saturations.